ACS Sustainable Chemistry & Engineering

pubs.acs.org/journal/ascecg

Research Article

Sulfonic Mesostructured SBA-15 Silicas for the Solvent-Free Production of Bio-Jet Fuel Precursors via Aldol Dimerization of Levulinic Acid

Marta Paniagua,* Florentina Cuevas, Gabriel Morales, and Juan A. Melero

Cite This: *ACS Sustainable Chem. Eng.* 2021, 9, 5952–5962

Read Online

ACCESS | Metrics & More | Article Recommendations | Supporting Information

ABSTRACT: Sulfonic acid-functionalized mesostructured silicas have been evaluated in the solvent-free aldol dimerization of biomass-derived levulinic acid into bio-jet fuel precursors. These compounds produce branched alkanes in a subsequent hydrodeoxygenation process, with suitable properties for being a renewable alternative to conventional fossil aviation fuels. The combination of activity and selectivity toward the desired condensation products achieved over sulfonic acid-functionalized SBA-15 materials is superior to those displayed by other commercial solid acid catalysts. Enhanced textural properties provided by the mesoporous SBA-15 support contribute to such improved catalytic performance. The strength and loading of the mesoporous silica-supported sulfonic acid moieties are also important factors affecting the catalytic performance of the materials. Reaction conditions (temperature, time, and catalyst loading) have been optimized for propylsulfonic acid-functionalized mesostructured silica (Pr-SBA-15) by means of a response surface methodology, leading to a maximum yield to levulinic acid dimerization products of 58.4% (145 °C, 0.15 g of catalyst, 24 h, no solvent). Under these reaction conditions, conversion of levulinic acid is 61.1%, indicating excellent selectivity toward bio-jet fuel precursors. A small catalytic activity decay has been detected in reutilization experiments, attributed to the formation of organic deposits onto the catalyst surface. A mild acid washing of the catalyst allowed a significant recovery of the initial activity.

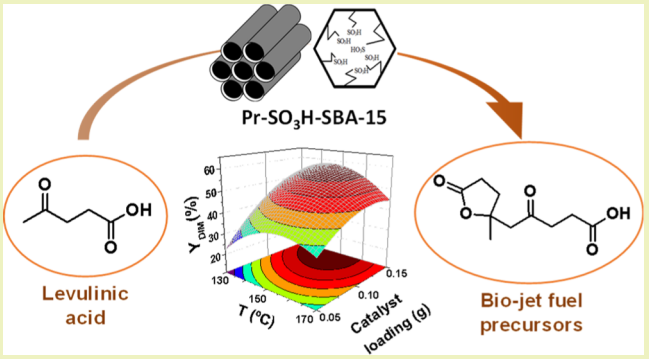

KEYWORDS: *bio-jet fuel, lignocellulose, levulinic acid, aldol dimerization, sulfonic acid, mesoporous silica*

INTRODUCTION

Transportation fuels are obtained mainly from conventional fossil fuels, this sector being responsible for approximately a quarter of world greenhouse gas (GHG) emissions. In particular, jet fuels account for around 6% of refined crude oil products and 2% of the total anthropogenic GHG emissions.[1] In 2016, in the European Union, this figure reached 3.6%, which corresponds to 13.4% of the emissions from transport, making aviation the second mode of transport in CO_2 emissions behind road traffic.[2] With the purpose of decreasing the GHG emissions for a sustainable future, many countries are adopting different key policies and measures, such as those described in "The European Green Deal," recently published by the European Commission (COM/2019/640).[3] Currently, no technology has been developed to move a commercial aircraft with any other alternative than liquid fuels, and although this could be feasible in the future, the aviation sector needs to focus on increasing fuel efficiency, as well as on the development of sustainable fuels. Hence, advanced biofuels appear as essential in the "hard-to-decarbonize" aviation transport in order to achieve the settled ambitious goals, such as those included in the new EU 2030 Climate Target Plan, to reduce GHG emissions by 55% in 2030 and to achieve complete decarbonization in 2050.

Biomass is the only renewable alternative to produce bio-jet fuel. Current technology enables the production of sustainable aviation fuels from a wide range of raw materials, including triglycerides, lignocellulosic biomass, sugars, and starchy feedstock.[4] Among the different raw materials, lignocellulosic biomass has a high potential since it is the most abundant and widely accessible form of biomass on earth, being also a low-cost feedstock, in particular, residual biomass from agriculture and forestry. There are different routes to convert lignocellulosic biomass into liquid fuels by thermochemical processes: pyrolysis, gasification, and hydrothermal upgrading. Among them, gasification of biomass into syngas followed by

Received: January 18, 2021
Revised: February 27, 2021
Published: April 16, 2021

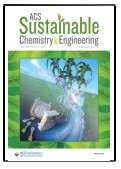

https://doi.org/10.1021/acssuschemeng.1c00378
ACS Sustainable Chem. Eng. 2021, 9, 5952–5962

Scheme 1. Reaction of Self-Aldol Condensation of LA and the Main Dimerization Products Detected in the Product Mixture: (a) Tetrahydro-2-methyl-5, γ-Dioxo-2-furanpentanoic Acid; (b) 3-(2-Methyl-5-oxotetrahydrofuran-2-yl)-4-oxopentanoic Acid; (c) 3-Acetyl-2-methyltetrahydro-5-oxo-2-furanpropanoic Acid[21]

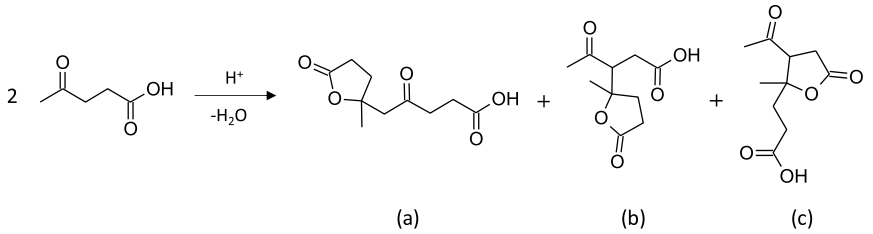

the Fischer−Tropsch process is one of the certified pathways by ASTM for the production of aviation biofuel for commercial use, and it can be blended up to 50% v/v with fossil jet fuel.[5] However, the thermochemical pathway for the processing of biomass involves high energy consumption.[4] In this context, the direct catalytic routes for the conversion of lignocellulose to aviation fuel-range hydrocarbons have recently received considerable attention due to the mild reaction conditions and the possibility of reaching high selectivity to the desired products.[6−8] The controlled depolymerization of cellulose and hemicellulose leads to the production of monosaccharides that can be processed through dehydration reactions, leading to the production of platform molecules such as 5-hydroxymethyl-furfural, furfural, and levulinic acid (LA) that might play the role of cornerstone components for the deployment of commercial-scale biorefineries.

Among these platform molecules, LA has been identified as one of the 12 promising building block chemicals by the US Department of Energy due to its high versatility to be transformed into a great variety of high-value bio-based chemicals, materials, or biofuels.[9,10] It can be efficiently obtained from cellulosic biomass with yields close to 80 mol %, based on hexose content, through a continuous hydrolytic process such as Biofine or Dibanet.[11,12] On the industrial scale, several companies are developing industrial processes aiming for the large-scale production of LA with a significant focus given to some commercial applications of LA.[13]

In order to obtain aviation fuel-range hydrocarbons from LA, since it has only five carbon atoms, increasing the carbon chain length by C−C coupling reactions of two or more LA molecules is necessary. In this sense, LA has two reactive functional groups, a ketone and a carboxylic acid group, through which direct self-condensation reactions could proceed by aldol condensation and ketonization, respectively.[14] Ketonization of two LA molecules provides the intermediate oxygenated adduct, 2,5,8-nonatrione, which can be further converted by a hydrodeoxygenation process to yield the linear C9 hydrocarbon nonane as the final compound.[15] This reaction is promoted by metal oxides and zeolites, and most of them are carried out in the gas phase under relatively high temperatures (473−673 K).[16] Under such conditions, the product of the direct ketonization of LA is highly reactive, thus decreasing the selectivity to the final desired product. On the other hand, this route provides linear alkanes with lower octane number and higher freezing points than the corresponding branched alkanes. Hence, they cannot be used directly as aviation fuel without previous hydroisomerization.[17]

Besides ketonization, LA can undergo self-aldol condensation reactions producing C10 oxy-compounds (Scheme 1). These compounds fall within the range of jet fuel, and after hydrodeoxygenation, they produce branched alkanes. Only a few studies on this alternative for carbon-chain increasing reactions from LA have been reported in the literature.[18−21] The dimerization of LA can be accomplished via base catalysis under mild conditions using mixed Mg-based oxides as catalysts.[19] Bulk MgZr oxides showed a good balance of stability and base−acid activity. However, only low conversions could be obtained—33% after 24 h—since the presence of the carboxylic group in LA can neutralize/deactivate base catalytic sites, leading to low efficiencies. Therefore, a more suitable alternative to develop this process could be the use of an acid catalysis system. Recently, a homogeneous catalytic system has been studied combining Lewis and Brønsted acidity, discovering the existence of a synergistic effect between both types of acids. With this reaction system, the above-mentioned deactivation by the acid is inhibited, leading to higher yields of the condensed products. Using the combination of $ZnCl_2$ (15 mol %) and trichloroacetic acid (5 mol %) as Lewis and Brønsted acid catalysts respectively, LA conversions of 60% and yields to dimerization products of 51% were achieved at 130 °C.[20] More recently, Amarasekara et al. studied the dimerization of LA using solid catalysts based on sulfonic groups supported on different amorphous siliceous and polymeric supports.[21] They obtained 56% yield over SiO_2−SO_3H, a catalyst that could be reused in consecutive reactions with only a slight decay in activity.

Organosulfonic acid-modified SBA-15 mesoporous materials with strong acidity, high specific surface area, well-ordered mesoporosity, and high thermal stability have been shown in the last decades to be able to carry out different acid-catalyzed reactions in the processing of bulky substrates. These materials have been tested in several catalytic transformations of biomass-derived compounds into added-value products, all of them with excellent catalytic performance in terms of both activity and selectivity to the target products.[22−25]

Therefore, within this contribution, the solvent-free aldol dimerization of LA for the production of bio-jet fuel precursors was carried out, for the first time, over different sulfonic acid-modified SBA-15 catalysts. The excellent properties of these materials and the feasibility of tuning the acid strength, the acid capacity, and the surface hydrophilic/hydrophobic balance of the sulfonic-modified SBA-15 silicas make these materials promising catalysts to be used in the valorization of biomass[26] and, specifically, in the self-aldol condensation of LA in which bulky molecules are involved. These materials have been benchmarked with other sulfonic commercial catalysts, correlating their physicochemical properties with the catalytic phenomena. A multivariable analysis has been used to assess the optimal conditions—temperature and catalyst loading—that yield the best results in terms of LA conversion and yield

https://doi.org/10.1021/acssuschemeng.1c00378
ACS Sustainable Chem. Eng. 2021, 9, 5952−5962

Table 1. Physicochemical, Textural, and Acidity-Related Properties for Sulfonic Acid-Modified Mesostructured SBA-15 Silicas

	textural properties			acid properties			
				acid capacity[c] (mequiv H^+/g)			
sample	pore size[a] (Å)	BET area (m^2/g)	pore volume[b] (cm^3/g)	sulfur	titration	accessibility[d] (%)	density[e] (μequiv H^+/m^2)
Pr-SBA-15 (5)	96	663	1.25	0.54	0.43	80	0.6
Pr-SBA-15 (10)	88	772	1.29	1.10	1.10	100	1.4
Pr-SBA-15 (15)	23	673	0.52	1.62	1.70	100	2.5
Ar-SBA-15 (5)	96	787	1.15	0.64	0.70	100	0.9
Ar-SBA-15 (10)	87	751	0.88	1.00	1.09	100	1.4
Ar-SBA-15 (15)	18	440	0.28	1.63	1.53	94	3.5

[a]Mean pore size from the adsorption branch applying the BJH model. [b]Total pore volume taken at P/P_0 = 0.975 as a single point. [c]Acid capacity defined as mequiv of acid centers per g of the catalyst (obtained either directly by titration or indirectly from sulfur content by elemental analysis). [d]Accessibility defined as the ratio between H^+ from acid−base titration and the sulfur content from elemental analysis. [e]Density defined as the ratio between mequiv of H^+ from acid−base titration and the surface area.

toward the dimerization products. Finally, the reusability of the catalyst after several reaction cycles has also been evaluated.

EXPERIMENTAL SECTION

Catalyst Preparation. Propylsulfonic acid-functionalized mesostructured silicas (Pr-SBA-15) were synthesized following the procedure described by Margolese et al.[27] For the synthesis of the catalysts, Pluronic 123 was used as the template block-copolymer ($EO_{20}PO_{70}EO_{20}$, Sigma-Aldrich), tetraethylorthosilicate (TEOS, Sigma-Aldrich, 98% purity) as the silica precursor, and (3-mercaptopropyl)trimethoxysilane (MPTMS, Sigma-Aldrich, 95% purity) as the sulfonic acid precursor. Arenesulfonic-acid functionalized mesostructured silicas (Ar-SBA-15) were synthesized following a previously reported procedure.[28] For this catalyst, Pluronic 123 was used as the template block-copolymer, TEOS as the silica precursor, and 2-(4-chlorosulfonylphenyl)ethyltrimethoxysilane (CSPTMS, Abcr GmbH, 50% purity) as the sulfonic acid precursor. In both cases, the amount of sulfur precursors (MPTMS and CSPTMS) has been selected to provide 5, 10, and 15% of total silicon atoms, and the catalysts were denoted as Pr-SBA-15 (5), Pr-SBA-15 (10), and Pr-SBA-15 (15), respectively, for propylsulfonic acid-functionalized mesostructured silicas, and Ar-SBA-15 (5), Ar-SBA-15 (10), and Ar-SBA-15 (15), respectively, for arenesulfonic-acid functionalized mesostructured silicas. The molar composition in the synthesis media for each material is shown in Table S1. The synthesis strategy for the preparation of sulfonic acid-modified mesostructured materials is schematized in the literature.[29]

Catalyst Characterization. The textural properties of the sulfonic acid-modified mesostructured silicas were determined by nitrogen adsorption−desorption isotherms recorded at 77 K using a Micromeritics TriStar 3000 unit. Surface area was obtained using the Brunauer−Emmett−Teller (BET) method, pore size distributions were calculated through the Barrett−Joyner−Halenda (BJH) method using the Kruk−Jaroniec−Sayari correction, and the total pore volume was taken at P/P_0 = 0.975. Structural ordering was obtained by means of X-ray powder diffraction (XRD) patterns acquired on a Philips X'Pert diffractometer using the Cu Kα line. Data were recorded from 0.6 to 5° (2θ) with a resolution of 0.02°. The number of acid sites was potentiometrically assessed by titrating a suspension of 0.05 g of acid catalyst in 15 g of 2 M NaCl (aq) with 0.01 M NaOH (aq). Sulfur content was determined by means of elemental analysis (Flash 2000 Organic Elemental Analyzer, from Thermo Scientific), and total organic content was determined through thermogravimetric analysis (SDT 2960 Simultaneous DSC−TGA, from TA Instruments) with an air flow rate of 100 mL/min and a heating ramp of 5 °C/min.

Furthermore, as reference catalysts, commercial acid catalysts were also evaluated in this work. Acidic macroporous resin, Amberlyst-15, and a homogeneous catalyst, *p*-toluenesulfonic acid (PTSA), were supplied by Sigma-Aldrich. SAC-13 nanocomposite, a perfluorosulfonic acid resin supported on silica (Nafion-SiO_2), was purchased from DuPont, and the nonstructured amorphous silicas, propylsulfonic acid-modified silica (Pr-SiO_2), and tosic acid-modified silica (Ar-SiO_2) were obtained from SiliaBond.

Reaction Procedure. Based on the proposed mechanism for solid acid-catalyzed aldol dimerization of LA reported by Amarasekara et al.,[21] Scheme 1 is a representation of the self-aldol condensation reaction of LA, showing the main dimerization products: tetrahydro-2-methyl-5, γ-dioxo-2-furanpentanoic acid (a); 3-(2-methyl-5-oxotetrahydrofuran-2-yl)-4-oxopentanoic acid (b); 3-acetyl-2-methyltetrahydro-5-oxo-2-furanpropanoic acid (c). The three dimers are interesting as precursors for the production of bio-jet fuel through subsequent hydrodeoxygenation reaction, so they have been pooled together herein as desired dimerization products (DIM).

Reaction runs were performed in ACE pressure glass reactors immersed in an oil bath under temperature control and continuous magnetic stirring. After the specific reaction time, the tube reactor was removed from the oil bath and the sample was analyzed. Typically, the composition of the reaction mixture was 1.16 g (10 mmol) of LA (Sigma-Aldrich, 98% purity), 0.1 g of sulfolane (Sigma-Aldrich, 99% purity) as the internal standard, and the respective mass of the catalyst. For catalyst screening, aldol dimerization of LA was performed up to 6 h at 130 °C, adding 0.1 g of the catalyst. For the optimization of reaction conditions, the reaction variables investigated were temperature (130−190 °C), reaction time (0−24 h), and catalyst loading (0.05−0.15 g). Thereafter, under the optimized reaction conditions, a reusability study was carried out.

Product Analysis. Reaction samples were analyzed combining gas chromatography (GC) and nuclear magnetic resonance (NMR) spectroscopy. From the reaction mixture, 0.2 mL was taken and dissolved in deuterated chloroform, filtered to remove the catalyst, and analyzed by means of ^{1}H NMR in a Varian Mercury Plus spectrometer operating at 400 MHz. Dimerization products were identified and calculated based on these analyses by comparison with published NMR data and following the same calculation procedure to that reported in the literature.[20,21] A representative ^{1}H NMR spectrum of the reaction mixture is shown in Figure S1. The remaining nonreacted LA in the reaction media was analyzed by GC, after first diluting the reaction mixture with acetone, using a Varian 3900 gas chromatograph equipped with an Agilent CP-WAX 52 CB column (30 m × 0.25 mm, DF = 0.25 μm) and a flame ionization detector. LA quantification was based on the calibration of the GC analysis unit with a standard stock solution of pure commercially available chemical using sulfolane as the internal standard. A representative GC chromatogram of the reaction mixture is shown in Figure S2. Catalytic results are shown either in terms of conversion of LA (X_{LA}) or in terms of yields (Y_{DIM}) and selectivity (S_{DIM}) toward the pooled dimerization products shown in Scheme 1 (eqs 1−3). Moreover, two additional parameters have been defined to help in the discussion of the catalytic phenomena: the specific productivity (SP) of the desired products per acid site (SP, eq 4) and the catalyst

https://doi.org/10.1021/acssuschemeng.1c00378
ACS Sustainable Chem. Eng. 2021, 9, 5952−5962

Table 2. Physicochemical Properties Corresponding to Commercial Sulfonic Acid-Based Catalysts[a]

catalyst	acid capacity (mequiv H^+/g)	BET area (m^2/g)	pore size (Å)	pore volume (cm^3/g)	density (μequiv H^+/m^2)
Amberlyst-15	≥4.70	45	300	0.40	104
Pr-SiO_2	1.04	301[b]	20−200[b]	0.44	3.4
Ar-SiO_2	0.78	279[b]	20−200[b]	0.38	2.8
Nafion-SiO_2	0.12	>200	>100	0.60	0.6
PTSA	5.80				

[a]Properties provided by the suppliers. [b]Experimentally determined by N_2 adsorption−desorption isotherms at 77 K.

productivity (CP) defined as the grams of desired products formed per gram of the catalyst (CP, eq 5).

$$X_{LA} = \frac{\text{reacted mol of LA}}{\text{initial mol of LA}} \times 100 \quad (1)$$

$$Y_{DIM} = \frac{2\cdot\text{formed mol of dimerization products}}{\text{initial mol of LA}} \times 100 \quad (2)$$

$$S_{DIM} = \frac{2\cdot\text{formed mol of dimerization products}}{\text{reacted mol of LA}} \times 100 \quad (3)$$

$$SP = \frac{\text{formed mmol of dimerization products}}{\text{acid capacity (meq } H^+/g)} \quad (4)$$

$$CP = \frac{\text{formed grams of dimerization products}}{\text{grams of catalyst}} \quad (5)$$

RESULTS AND DISCUSSION

Screening of Catalysts. To check the influence of the catalytic system, screening of different sulfonic acid-modified solids was performed. The aim of this preliminary study is to correlate the catalytic properties such as porous structure and acid site strength and concentration with their catalytic activity in the solvent-free aldol dimerization of LA, in terms of LA conversion toward the desired products.

Table 1 summarizes the most relevant physicochemical properties recorded for the sulfonic acid-modified mesostructured catalysts tested in this work. Data from XRD and nitrogen adsorption isotherms evidence high mesoscopic ordering (2D-hexagonal *p6mm* structure) and high surface areas along with narrow pore size distributions around 8−10 nm for the materials with 5 and 10% of sulfur precursor loading (Figures S3 and S4). However, at higher loadings of sulfonic acid groups [samples Pr-SBA-15 (15), and Ar-SBA-15 (15)], the formation of the mesostructure is hindered by the higher degree of organic loading, leading to lower BET surface area and pore volume. In addition, the TEM images shown in Figure S5 confirm the high mesoscopic order of the samples Pr-SBA-15 (10) and Ar-SBA-15 (10). These materials exhibit a hexagonal array of uniform channels with the typical honeycomb appearance of SBA-15 materials.[30] Acid capacity was obtained either directly by titration or indirectly from sulfur content by elemental analysis. Note that all catalysts display high accessibility to the acid sites since the amount of mequiv H^+/g obtained from both analyses is very similar. In addition, the acid capacity can also be inferred from the corresponding weight losses determined via thermogravimetric analyses, showing again a fair agreement with the data shown in Table 1 (Figure S6). It is important to note that in the literature, a similar acid capacity was obtained using larger exchange cations such as TMA^+ and TEA^+ compared to the value using Na^+ cations, which is a strong indication that the sulfonic groups are located on the surface of mesopore walls, and hence, they will be accessible by LA during the dimerization reaction.[28]

Table 2 shows the most relevant physicochemical properties corresponding to the used commercial sulfonic acid-based catalysts, most of them being provided by the suppliers.

Figure 1 depicts the LA conversion as well as the yield to the dimerization products achieved over each catalyst. Reaction

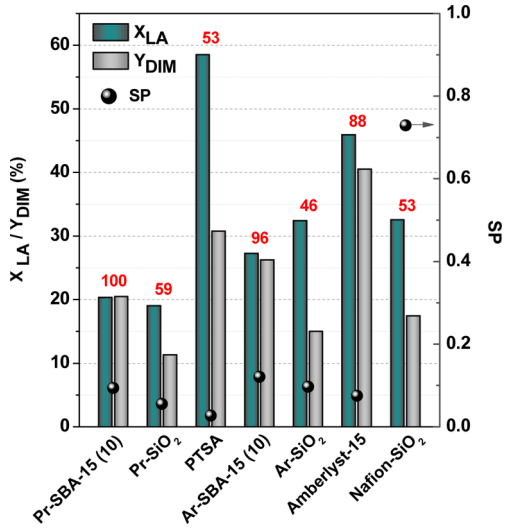

Figure 1. LA conversion and yield to dimerization products over sulfonic acid-modified catalysts (left axis). SP (right axis). Selectivity (%) toward the dimerization products: numbers in red. Reaction conditions: LA, 10 mmol; reaction time, 6 h; temperature, 130 °C; catalyst loading, 0.1 g.

conditions for this study were fixed as follows: temperature 130 °C, catalyst loading 0.1 g, and reaction time 6 h. These starting conditions have been selected based on the literature.[21] Catalysts assayed in this screening have included the synthesised propyl- and arene-sulfonic acid-modified SBA-15 mesoporous silicas with 10 mol % SO_3H loading, Pr-SBA-15 (10) and Ar-SBA-15 (10). These materials were benchmarked with sulfonic commercial catalysts. Additionally, a homogenous sulfonic acid catalyst (PTSA) has also been included as reference for comparison purposes. As a reaction control, a blank in the absence of the catalyst was performed, giving null LA conversion after 6 h. This indicates that, under the tested reaction conditions, the extent of dimerization of LA via autocatalysis is negligible, so the presence of an acid catalyst, at least one more active than LA itself, is necessary to carry out the reaction.

In these kinds of catalysts, a relevant factor contributing to the catalytic activity, in terms of either conversion or selectivity, is usually the acid strength of the sulfonic acid sites. Taking this parameter into account, three groups of catalysts were assayed in this work, as introduced by the

https://doi.org/10.1021/acssuschemeng.1c00378
ACS Sustainable Chem. Eng. 2021, 9, 5952−5962

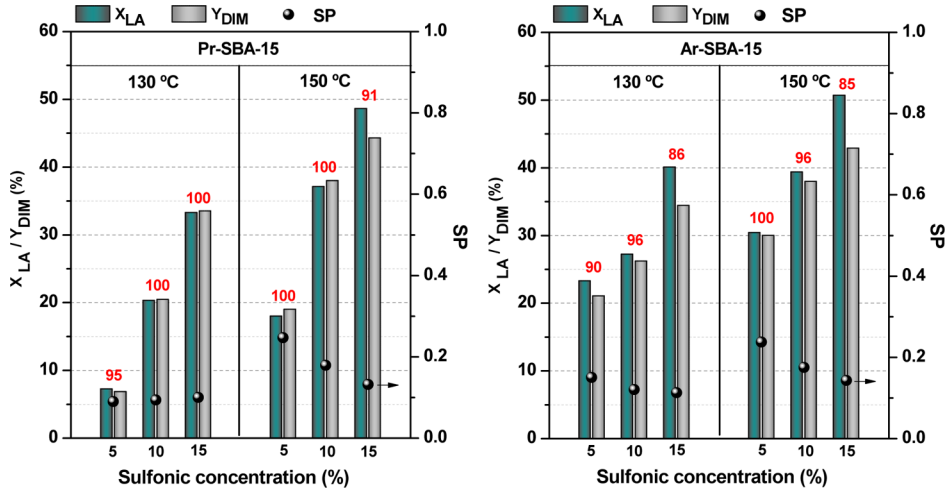

Figure 2. LA conversion and yield to dimerization products over sulfonic acid-modified SBA-15 catalysts (left axis). SP (right axis). Selectivity (%) toward the dimerization products: numbers in red. Reaction conditions: LA, 10 mmol; reaction time, 6 h; temperature, 130 and 150 °C; catalyst loading, 0.1 g.

different molecular environments of the sulfonic acid sites, whose acid strength can be sorted as follows: Pr-SO_3H < Ar-SO_3H < Nafion.[31] Thus, the alkyl nature of the tethering moiety in the propyl-sulfonic acid-modified catalysts [Pr-SBA-15 (10), and Pr-SiO_2] results in lower acid strength.[28] As shown in Figure 1, both catalysts provided similar LA conversion (around 20%), but a higher yield to desired dimerization products (DIM) was obtained for the material based on SBA-15, remarkably achieving 100% of selectivity. Since both silica-based catalysts display identical acid moieties with a similar acid capacity (1.04 and 1.10 mequiv H^+/g, Tables 1 & 2), this can be considered a clear indication of the benefit of introducing a mesostructured versus a nonordered support. The improvement in selectivity is hypothesized to be related to a better dispersion of the acid sites coupled with a preferential orientation of the LA molecules within the porous structure. In fact, the predominant dimer obtained is the linear one (tetrahydro-2-methyl-5, γ-dioxo-2-furanpentanoic acid, Figure S1), which would be the one preferentially formed in a pore arrangement with hexagonal symmetry such as that in a SBA-15 material.

On the other hand, Ar-SBA-15 (10), Ar-SiO_2, Amberlyst-15, and PTSA have chemically equivalent sulfonic acid sites, consisting of an aromatic ring directly attached to the SO_3H group. This series of catalysts showed higher activity in terms of LA conversion compared to the propylsulfonic acid-functionalized catalysts, which can be attributed to the inherently stronger sulfonic acid sites due to the electron-withdrawing effect introduced by the aromatic ring of the arenesulfonic group.[28] The homogeneous nature of PTSA, leading to a complete absence of diffusional limitations, makes it the most active catalyst, providing the highest conversion of LA (58%). However, the yield to dimerization products was only 31%, indicating that this catalyst strongly promotes side reactions leading to poor selectivity toward dimerization products. In addition, the SP is very low compared to the solid catalysts tested. These results justify the beneficial effect of supporting the sulfonic acid sites on a solid support. Indeed, comparing the silica-supported catalysts, the Ar-SBA-15 (10) material provides almost complete selectivity toward the desired products. Moreover, when the comparison is made in terms of SP, both Pr-SBA-15 (10) and Ar-SBA-15 (10) present higher values than the respective nonordered silica materials, Pr-SiO_2 and Ar-SiO_2. Again, the presence of well-ordered mesopores with narrow pore size distributions favors the progress of the aldol dimerization process, minimizing side reactions. In these materials, the high surface areas, together with the use of a cocondensation synthetic route, ensures an excellent surface dispersion of the anchored sulfonic groups, leading to moderate surface densities (1.4 μequiv H^+/m^2 in both materials, Table 1). On the contrary, in the nonordered silicas, the surface densities are much higher (2.8−3.4 μequiv H^+/m^2, Table 2), which can explain their increased activity for nondesired side reactions.

In turn, the commercial sulfonic acid resin Amberlyst-15, conventionally used in many acid-catalyzed processes, provided the highest LA conversion (46%) among the heterogeneous catalysts tested, accompanied by high selectivity toward the dimerization products although not complete (88%). This material displays the lowest specific surface area but the highest acid capacity. Thus, the detrimental effect of their comparatively reduced surface area is somewhat balanced out by a remarkably elevated surface density (104 μequiv H^+/m^2, Table 2). The organic resin nature of this catalyst most likely generates a swelling effect with LA (since the reaction is performed in solvent-free conditions), so the interaction of LA and the catalytic sites would be higher than expected for such a low surface area. However, it must be pointed out that the SP of Amberlyst-15 remains lower than the SP of the mesostructured materials. In addition, the thermal stability of this organic resin is limited (120 °C according to the manufacturer), which hinders its application in this reaction for prolonged time periods. Finally, despite its low acid capacity, Nafion-SiO_2 provides a high LA conversion. The presence of perfluorinated hydrocarbon backbone in the polymer Nafion, fluorine atoms being the highly electron-withdrawing moieties in the vicinity of the sulfonic acid group, makes this catalyst the one with the highest acid strength compared to the rest of the catalysts. In terms of SP per acid site, Nafion-SiO_2 shows an outstanding value. However, the higher acid strength appears to promote also nondesired side reactions as the selectivity toward the dimerization products is very low (53%).

https://doi.org/10.1021/acssuschemeng.1c00378
ACS Sustainable Chem. Eng. 2021, 9, 5952−5962

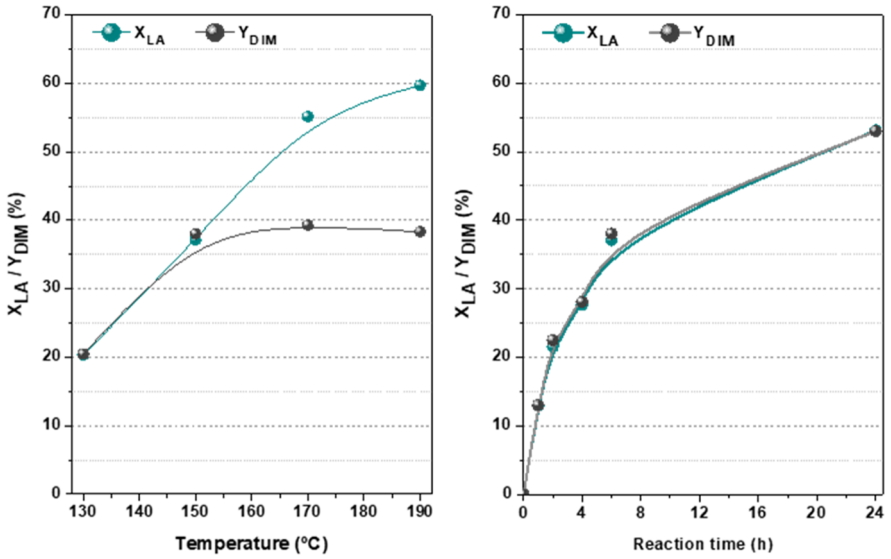

Figure 3. LA conversion and yield to dimerization products over Pr-SBA-15 (10). Effect of reaction temperature; reaction conditions: LA, 10 mmol; reaction time, 6 h; catalyst loading, 0.1 g (left side). Evolution with reaction time; reaction conditions: LA, 10 mmol; temperature, 150 °C; catalyst loading, 0.1 g (right side).

Therefore, SBA-15-supported catalysts showed excellent catalytic performances in terms of selectivity toward the desired condensation products, combined with a suitable conversion of LA under the screening conditions. Since this process is only the first step in the production of the final jet fuel hydrocarbons, selectivity in the dimerization of LA appears as a critical parameter to ensure adequate overall yields. In order to further analyse the behavior of these materials, the effect of the surface loading of propyl- and arene-sulfonic acid sites on the catalytic performance was next evaluated. Thus, SBA-15 catalysts with different concentrations of acid sites were synthesized and characterized (Table 1). Reaction conditions for this study were fixed as follows: temperature 130 and 150 °C, catalyst loading 0.1 g, and reaction time 6 h. The results are shown in Figure 2.

As the sulfonic acid site loading increases, the conversion of LA and the yield to the products of interest concomitantly increase. However, a progressive reduction of the selectivity to DIM is observed, especially for arenesulfonic acid-functionalized SBA-15, which might be attributed to its higher acid strength. The increase in temperature from 130 to 150 °C also affects positively the progress of the reaction, both in terms of LA conversion and DIM yields, for both types of catalysts. Analysing the SP, this parameter decreases as the concentration of acid sites on the catalysts increases, displaying the highest values for the materials with just 5 mol % of sulfonic groups (this decrease being more accentuated with the temperature). Since all catalysts in each series have the same type of acid site (propylsulfonic or arenesulfonic acid groups) supported on a mesostructured silica (SBA-15), this trend can be attributed to a better intrinsic catalytic performance of isolated acid sites. Actually, the SP values are inversely correlated with the surface concentration of sulfonic sites (Table 1, Figure S7).

In addition, for catalysts with 15% of sulfonic groups, as deduced from the textural properties calculated for these materials (Table 1, Figures S3, and S4), mesoscopic ordering is clearly flawed. Although they cannot be strictly considered a SBA-15 type silica, the nomenclature of the materials has been maintained. The high sulfonic acid concentration together with a reduction of the available surface area due to the lack of mesostructure provide both 15% materials with an excessive surface concentration of acid sites, eventually leading to the enhancement of side reactions. Thus, very close sulfonic groups could hinder each other to catalyse the formation of the bulky LA dimers, and other side reactions might be promoted instead, leading to an increase in LA conversion but also to a loss of selectivity toward the desired products.

Comparing SBA-15 catalysts functionalized with propylsulfonic and arenesulfonic acid groups, the former has higher selectivities than the latter in essentially every experiment (varying acid loading and temperature). This is attributed to a unique combination of excellent textural properties and moderate acid strength. Among the materials synthesized with propylsulfonic acid groups, Pr-SBA-15 (10) showed selectivities close to 100% for both temperatures, together with high yield to the desired adducts. As previously discussed, avoiding the promotion of side reactions in this system would be crucial for the overall production of jet fuel-range hydrocarbons. Therefore, this material was chosen for the following study of reaction condition optimization.

Preliminary Studies. As a previous step to the optimization of temperature and catalyst loading by means of experimental design methodology, preliminary studies were performed in order to establish the adequate range of reaction conditions. Figure 3 (left side) depicts the influence of reaction temperature on LA conversion and yield to dimerization products over Pr-SBA-15 (10).

As expected, an increase of the reaction temperature promotes a faster transformation of LA, as evidenced by the conversion of LA (around 20% at 130 °C and close to 60% at 190 °C). However, from the point of view of selectivity to dimerization products, there is an opposite effect: the higher the temperature, the lower the selectivity toward the desired adducts, indicating that side reactions are enhanced to a larger extent at high temperatures (larger activation energy), with the consequent reduction of the carbon balance and selectivity to DIM. Therefore, the best temperature would be 150 °C,

https://doi.org/10.1021/acssuschemeng.1c00378
ACS Sustainable Chem. Eng. 2021, 9, 5952−5962

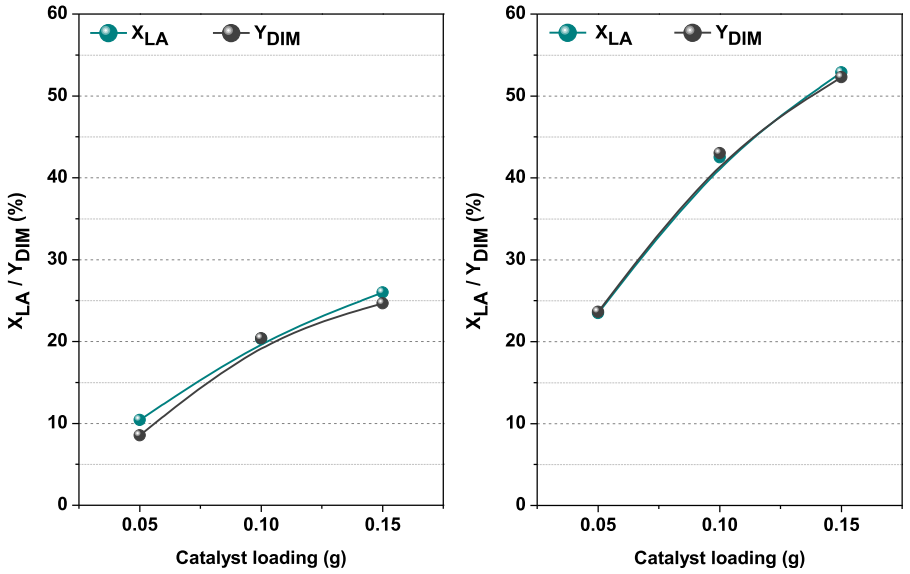

Figure 4. Effect of catalyst loading on LA conversion and yield to dimerization over Pr-SBA-15 (10). Reaction conditions: LA, 10 mmol; temperature, 130 °C; reaction time, 6 h (left side) and 24 h (right side).

resulting in 37% yield with 100% selectivity after 6 h. Under these conditions, the reaction time was also studied up to 24 h (Figure 3, right side). The conversion of LA increases with reaction time, and for all taken samples, the selectivity toward desired products remained close to 100%. A remarkable total yield close to 60% was obtained at 150 °C and 24 h, being the remainder of the mass balance unreacted LA (note that the reaction is being carried out under solvent-free conditions).

Additionally, the influence of the amount of catalyst was assessed for Pr-SBA-15 (10) at a moderate temperature of 130 °C for two different reaction times (6 and 24 h) (Figure 4). As shown, an increase in the catalyst loading produces an increase in both the LA conversion and the yield to DIM, achieving again selectivities close to 100% in all catalytic runs. Noteworthy, the same excellent behavior was observed after 24 h of reaction, even for the highest catalyst loading.

Statistical Analysis and Optimization. To optimize the main operating conditions affecting the LA conversion and the yield to dimerization products over the previously selected catalyst, Pr-SBA-15 (10), a factorial design and the response surface methodology were followed.[32] In this way, the most influential variables can be detected as well as the existence of interaction between them. A full 3^2 design (two factors and three levels for each one) was used to set the experimental design. Temperature and catalyst loading were selected as experimental factors since they are the most influential variables in this system. Reaction time was established at 24 h in order to achieve the highest values of yield attending to previous experiment (Figure 3). The levels chosen for temperature were 130, 150, and 170 °C, whereas the levels for catalyst loading were 0.05, 0.1, and 0.15 g (keeping a fixed amount of LA, 10 mmol). As response variables, the LA conversion (X_{LA}) and the yield to dimerization products (Y_{DIM}) were selected taking into account the main objective of achieving high conversion of LA and high yield to dimerization products while minimizing the formation of undesired byproducts. In addition, CP was also analysed since, from an industrial point of view, a potential key goal would be to maximize the amount of C10 dimers generated per gram of catalyst.

In this way, the standard experimental matrix for the design is shown in Table 3. Columns 2 and 3 represent the factor levels on a natural scale, whereas columns 4 and 5 represent the 0 and ±1 encoded factor levels on a dimensionless scale. Experiment corresponding to the central point of the design was repeated three times in order to determine the variability of the results and to assess the experimental error. Experiments were run at random to minimize the effect of possible systematic trends in the observed responses. The table also includes the experimental results of the response variables.

Table 3. Experiment Matrix and Experimental Results for the Dimerization of LA Over Propylsulfonic Acid-Modified Mesostructured Silica, Pr-SBA-15 (10)[a]

run number	T (°C)	C (g)	I_T	I_C	X_{LA} (%)	Y_{DIM} (%)	CP (g/g)
1	130	0.1	−1	0	42.5	43.0	4.6
2	150	0.05	0	−1	37.2	33.2	7.1
3	150	0.1	0	0	53.1	53.0	5.7
4	130	0.05	−1	−1	23.5	23.6	5.1
5	150	0.15	0	+1	62.2	59.8	4.3
6	150	0.1	0	0	53.7	54.5	5.8
7	150	0.1	0	0	52.8	51.7	5.5
8	170	0.05	+1	−1	43.1	34.1	7.3
9	150	0.1	0	0	53.9	52.7	5.6
10	170	0.15	+1	+1	80.1	43.4	3.1
11	130	0.15	−1	+1	52.9	52.3	3.7
12	170	0.1	+1	0	67.0	43.4	4.6

[a]Reaction conditions: LA, 10 mmol; reaction time, 24 h. Note: T, temperature; C, catalyst loading; I, coded value; X_{LA}, conversion of LA as (mmol of converted LA/mmol of starting LA) × 100; Y_{DIM}, yield to dimerization products as (2·formed mmol of dimerization products/mmol of starting LA) × 100; CP, catalyst productivity as grams of desired products formed/grams of catalyst.

From the matrix generated by the experimental data and assuming a second-order polynomial model, eqs 6−8 were obtained by multiple regression analysis. The statistical models are obtained from encoded levels giving the real influence of each variable on the process. To facilitate the interpretation of

https://doi.org/10.1021/acssuschemeng.1c00378
ACS Sustainable Chem. Eng. 2021, 9, 5952−5962

the equations, Figure 5 plots the response surfaces and contour plots of LA conversion, yield to dimerization products, and CP.

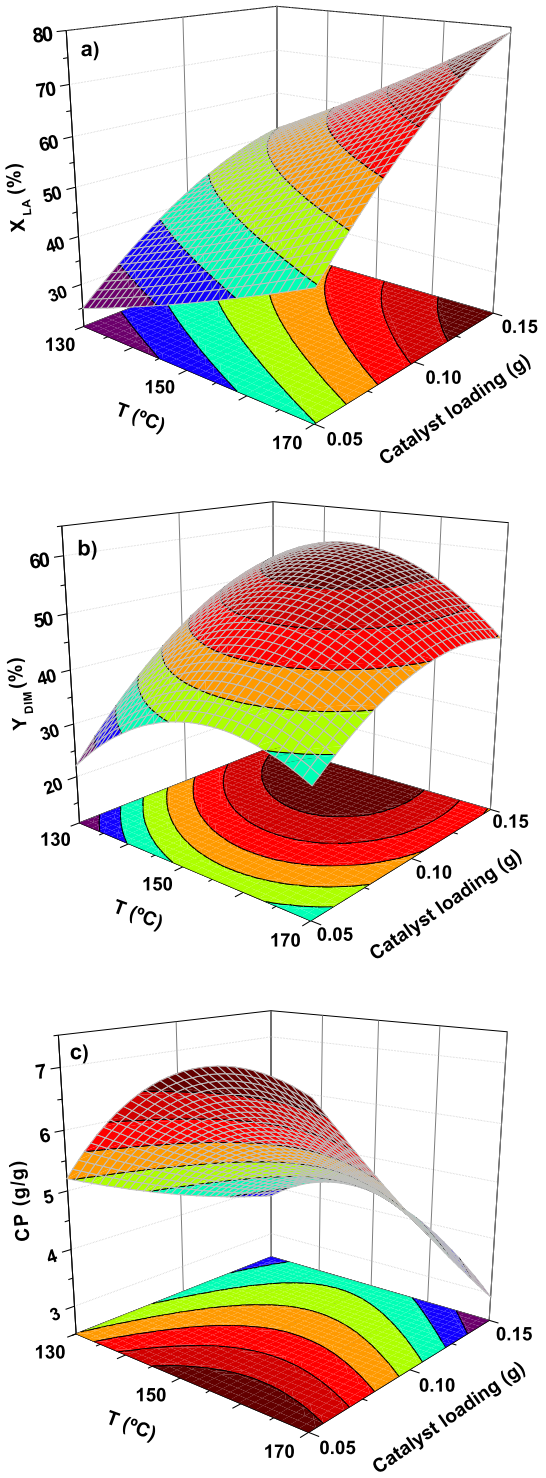

Figure 5. Response surfaces and contour plots of LA conversion (a), yield to dimerization products (b), and CP (c) over Pr-SBA-15 (10). Reaction conditions: LA, 10 mmol; reaction time, 24 h.

$$X_{LA} = 53.5708 + 11.8833I_T + 15.2333I_C + 0.7875{I_T}^2 + 1.9I_TI_C - 4.2625{I_C}^2 \quad (r^2 = 0.989) \tag{6}$$

$$Y_{DIM} = 52.7042 + 0.333333I_T + 10.7667\,I_C - 8.9625{I_T}^2 - 4.85I_TI_C - 5.6625{I_C}^2 \quad (r^2 = 0.980) \tag{7}$$

$$CP = 5.625 + 0.266667I_T - 1.4I_C - 0.975{I_T}^2 - 0.7I_TI_C + 0.125{I_C}^2 \quad (r^2 = 0.984) \tag{8}$$

An evaluation of the regression error was performed on these models to validate their use for making predictions. An indication of the goodness of the fit is the high values recorded for the regression coefficients (r^2). All of them are over 0.98, which indicates a very high correlation between the experimentally observed results and the predicted values by mathematical models. Indeed, the good agreement between experimental and predicted values can be easily visualized in Figure 6. Furthermore, reproducibility of the experimental system is elevated, as evidenced by the arithmetical averages and standard deviations calculated from the central-point replicas: LA conversion (53.4 ± 0.5%); yield to DIM (53.0 ± 1.2%); CP (5.7 ± 0.1). All standard deviations were below 2% so that the experimental error is small, and it does not affect the validity of the conclusions obtained from the interpretation of the models.

Analysis of variance was performed to check the parameter estimation and the goodness of the model fitting. The test of statistical significance was based on the total error criteria with a confidence level of 95.0%. The significance of each parameter in the model can be assessed from its *P*-value. In this way, the statistical analysis in the studied experimental range identifies the linear terms of the model, I_C and I_T, as the most important factors in the LA conversion response. Both of them have a positive effect, which means that an enhancement of the temperature and catalyst loading produces an increase in the conversion of LA, independently of the value of the other factor. In contrast, the quadratic effect of catalyst loading has a significant negative influence on the LA conversion, indicating that the increase of this variable does not produce a constant rise in LA conversion because of the significant curvature effect observed at high values of these variables. Figure S8a shows the standardized Pareto chart for this response, evidencing the significant factors as described above. Figure 5a includes the response surface and contour plots of LA conversion corresponding to eq 6 and clearly shows the above-mentioned effect of both factors: the gradual increase of both reaction variables enhances the conversion of LA. Thus, from the point of view of LA conversion, the optimal values under the range of study would be the highest temperature (170 °C) and the highest catalyst loading (0.15 g), which correspond to the experiment (+1, +1) of the experimental design. At these conditions, LA conversion predicted by the nonlinear model (eq 6) is 79.1% and the experimental result is 80.1%, in fair agreement with the model prediction.

In the case of yield to dimerization products (eq 7, Figures S8b, and 5b), the catalyst loading is identified as the most significant factor, having an overall positive effect on this response. Equation 7 also revealed an important contribution of the quadratic terms ${I_T}^2$, ${I_C}^2$, and I_TI_C, resulting in a significant curvature of the model, clearly evidenced by the shape of the response surface represented in Figure 5b. This is an indication of the necessity of evaluating the factors all together in order to account for the interactions between them. As a result, the model gave the maximum predicted value for the yield in the studied range as 58.4%, which corresponds to

https://doi.org/10.1021/acssuschemeng.1c00378
ACS Sustainable Chem. Eng. 2021, 9, 5952−5962

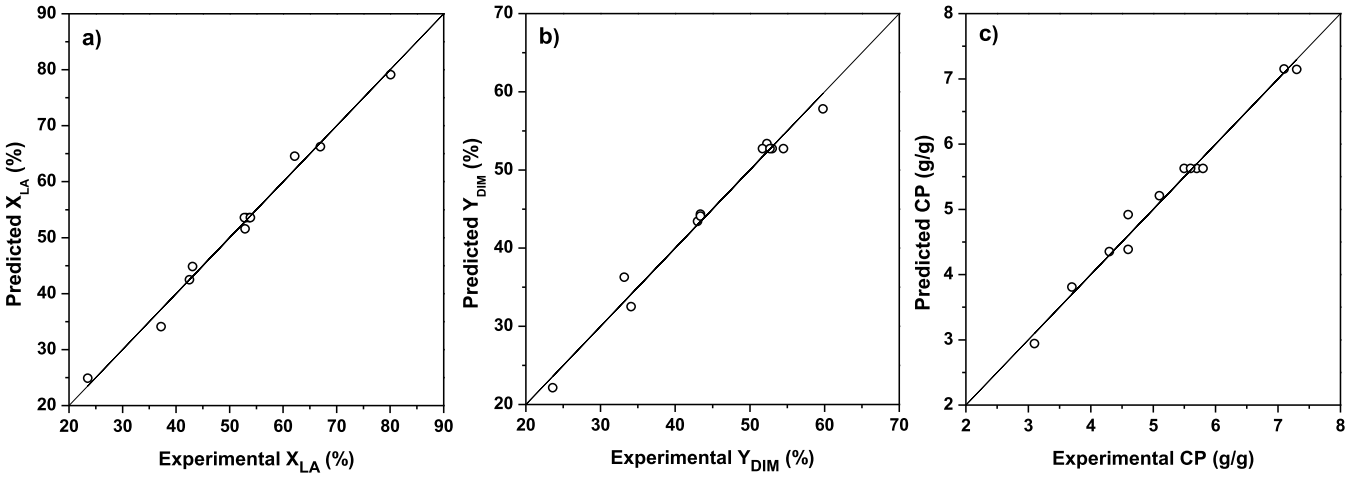

Figure 6. Experimental vs predicted values for LA conversion (a), yield to dimers (b), and CP (c). Reaction conditions: catalyst, Pr-SBA-15 (10); LA, 10 mmol; reaction time, 24 h.

the following reaction conditions: 145 °C and 0.15 g of catalyst (I_T = −0.25, I_C = +1, in coded values). At these reaction conditions, the model predicted an LA conversion of 61.1%, indicating that the predicted selectivity toward the dimerization products is very high (95.6%). Therefore, these reactions conditions would be optimal in order to maximize the production of dimerization products from LA without the promotion of other side reactions.

However, from a more industrial point of view, it is important to optimize the catalyst usage, and therefore, the CP was also analysed and modelled as a function of the temperature and catalyst loading (eq 8, Figures S8c, and 5c). The coefficients in eq 8 identify the linear term of catalyst loading as the most significant factor in the CP response. As expected, this factor has a negative effect on this variable response since an increase in the catalyst loading produces a decrease in CP. In addition, the quadratic effect of temperature and the temperature-catalyst loading interaction have a significant negative influence on the CP. Figure 5c shows that the increase in the temperature does not produce a constant rise in the CP, with a significant curvature effect. Also, the influence of catalyst loading in the response is strongly dependent on temperature: at high temperatures, an increase of the catalyst loading yields a decrease in CP, whereas at low temperatures, the effect of catalyst loading becomes much less significant. Thus, the model predicted the highest CP at the lowest catalyst loading (0.05 g) and a high temperature (160 °C), reaching a CP value of 7.4 while keeping the high selectivity of the process. However, under such reaction conditions, the yield to dimerization products predicted by the model would be limited to 36.3%. Note that it should be necessary to perform a techno-economic analysis on the overall production process (reaction and separation units) in order to identify the best option: working at the optimal CP or at the optimal yield to dimers.

Catalyst Reusability and Stability. Additionally, aiming to evaluate the reusability of the Pr-SBA-15 (10) catalyst in this reaction system, recycling tests were conducted for three consecutive reaction cycles at the optimal conditions to maximize the production of dimerization products from LA without the promotion of other side reactions (145 °C and 0.15 g of catalyst). Figure 7 displays the obtained results in terms of LA conversion and yields to dimerization products.

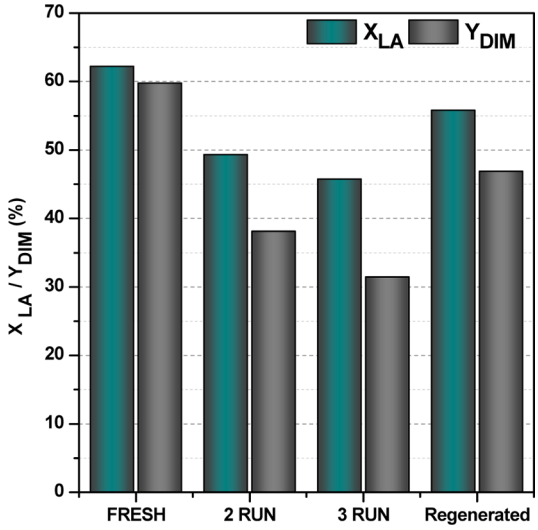

Figure 7. Reusability of catalyst Pr-SBA-15 (10) on the dimerization of LA. Reaction conditions: LA, 10 mmol; temperature, 145 °C; catalyst loading, 0.15 g; reaction time, 24 h.

Catalyst recovery between consecutive runs was carried out by simple filtration without any further treatment. Using such a simple procedure, a progressive loss of activity is observed both in terms of LA conversion and yield to desired products. Spent catalysts were analysed by means of elemental analysis and thermogravimetric analysis in order to evaluate the formation of organic deposits or the leaching of sulfur species as the most plausible deactivation causes. Elemental analysis (Table S2) evidenced a decrease in the sulfur content (from 1.3 to 0.9 mmol S/100 g of SiO_2) together with an increase in the carbon content (from 5.9 to 20.5 wt %). The results of the thermogravimetric analysis of the spent catalyst corroborate the increase of total organic content in the catalyst (Figure S9). These results point out to a partial loss of sulfur sites and to the deposition of organic carbonaceous byproducts on the catalyst surface. Taking into account that in the first run the selectivity is almost 100%, such deposits would come mainly from the dimerization products remaining adsorbed on the catalyst surface as no solvent is used in the reaction. The spent catalyst after three catalytic cycles (145 °C and 24 h each) was then regenerated by washing with a solution of 0.05 M HCl in

https://doi.org/10.1021/acssuschemeng.1c00378
ACS Sustainable Chem. Eng. 2021, 9, 5952−5962

ethanol, keeping under reflux during 4 h. Results shown in Figure 7 indicate that the catalytic performance is significantly recovered, from 32% of DIM yield to 47%. The mild acid-washing regeneration step seems to be able to remove the organic deposits placed onto the catalyst surface, the loss of the labile fraction of SO_3H groups being the main cause for the not full recovery of the catalytic performance.

CONCLUSIONS

Sulfonic acid-functionalized mesostructured materials have demonstrated excellent catalytic behavior in the solvent-free dimerization of LA to yield precursors for bio-jet fuel. Their activity and selectivity have been shown to be superior to other conventional acid catalysts due to the better accessibility and dispersion of the acid sites. The acid strength of the catalytic sites has also been shown to be a determinant parameter in the catalytic performance since the use of stronger acid centers, such as those in arenesulfonic acid and perfluorosulfonic acid sites, also promotes side reactions, decreasing the selectivity to the desired products. Pr-SBA-15 (10) material is shown as an active and selective catalyst in the solvent-free LA dimerization due to an optimal combination of textural properties, moderate strength, and surface density of the propilsulfonic acid groups. The experimental design model carried out for different levels of temperature and catalyst loading has shown that it is necessary to use high catalyst loading (0.15 g) and moderate temperature (145 °C) in order to achieve high yield and selectivity toward the dimerization products. Under these reaction conditions, LA conversions of 61.1% and yield to dimerization products of 58.4% were achieved after 24 h. Moreover, the catalytic performance of these sulfonic mesostructured materials was significantly recovered after a mild acid-washing regeneration step.

ASSOCIATED CONTENT

Supporting Information

The Supporting Information is available free of charge at https://pubs.acs.org/doi/10.1021/acssuschemeng.1c00378.

Detailed catalyst preparation and characterization, reaction procedure, product analysis, SP versus SO_3H surface concentration, and spent catalyst characterization (PDF)

AUTHOR INFORMATION

Corresponding Author

Marta Paniagua − *Chemical and Environmental Engineering Group, ESCET, Universidad Rey Juan Carlos, 28933 Madrid, Spain;* orcid.org/0000-0002-2485-5121; Phone: +34 91 488 73 67; Email: marta.paniagua@urjc.es

Authors

Florentina Cuevas − *Chemical and Environmental Engineering Group, ESCET, Universidad Rey Juan Carlos, 28933 Madrid, Spain*

Gabriel Morales − *Chemical and Environmental Engineering Group, ESCET, Universidad Rey Juan Carlos, 28933 Madrid, Spain;* orcid.org/0000-0002-5070-4749

Juan A. Melero − *Chemical and Environmental Engineering Group, ESCET, Universidad Rey Juan Carlos, 28933 Madrid, Spain*

Complete contact information is available at: https://pubs.acs.org/10.1021/acssuschemeng.1c00378

Author Contributions

The manuscript was written through contributions of all authors. All authors have given approval to the final version of the manuscript.

Notes

The authors declare no competing financial interest.

ACKNOWLEDGMENTS

The funding support from the Spanish Ministry of Science, Innovation and Universities, grant number RTI2018-094918-B-C42, the Regional Government of Madrid, grant numbers P2018/EMT-4344 (BIOTRES) and PEJ-2018-AI/AMB-11568, and the University Rey Juan Carlos (Young Researchers R&D Project ref. M2181-BIOCAVI) is kindly acknowledged.

REFERENCES

(1) ATAG. *Beginner's Guide to Sustainable Aviation Fuel*, November 1−24, 2017.

(2) *European Aviation Environmental Report*, 2019.

(3) European Commission. *The European Green Deal—COM (2019) 640*, 2019.

(4) Gutiérrez-Antonio, C.; Gómez-Castro, F. I.; de Lira-Flores, J. A.; Hernández, S. A Review on the Production Processes of Renewable Jet Fuel. *Renewable Sustainable Energy Rev.* **2017**, *79*, 709−729.

(5) Prussi, M.; O'Connell, A.; Lonza, L. Analysis of Current Aviation Biofuel Technical Production Potential in EU28. *Biomass Bioenergy* **2019**, *130*, 105371.

(6) Wang, H.; Yang, B.; Zhang, Q.; Zhu, W. Catalytic Routes for the Conversion of Lignocellulosic Biomass to Aviation Fuel Range Hydrocarbons. *Renewable Sustainable Energy Rev.* **2020**, *120*, 109612.

(7) Nakagawa, Y.; Tamura, M.; Tomishige, K. Recent Development of Production Technology of Diesel- and Jet-Fuel-Range Hydrocarbons from Inedible Biomass. *Fuel Process. Technol.* **2019**, *193*, 404−422.

(8) Li, H.; Riisager, A.; Saravanamurugan, S.; Pandey, A.; Sangwan, R. S.; Yang, S.; Luque, R. Carbon-Increasing Catalytic Strategies for Upgrading Biomass into Energy-Intensive Fuels and Chemicals. *ACS Catal.* **2018**, *8*, 148−187.

(9) Werpy, T.; Petersen, G. *Top Value Added Chemicals from Biomass*, 2004.

(10) Xue, Z.; Liu, Q.; Wang, J.; Mu, T. Valorization of Levulinic Acid over Non-Noble Metal Catalysts: Challenges and Opportunities. *Green Chem.* **2018**, *20*, 4391−4408.

(11) Hayes, D. J.; Fitzpatrick, S.; Hayes, M. H. B.; Ross, J. R. H. The Biofine Process—Production of Levulinic Acid, Furfural, and Formic Acid from Lignocellulosic Feedstocks. *Biorefineries-Industrial Processes and Products: Status Quo and Future Directions*; Wiley-VCH Verlag GmbH, 2008; Vol. *1*, pp 139−164.

(12) Final, D.; Summary, P. *DIBANET Final Publishable Summary Report July 2013*; 2013.

(13) Morales, G.; Melero, J. A.; Iglesias, J.; Paniagua, M.; López-Aguado, C. From levulinic acid biorefineries to γ-valerolactone (GVL) using a bi-functional Zr-Al-Beta catalyst. *React. Chem. Eng.* **2019**, *4*, 1834−1843.

(14) Käldström, M.; Lindblad, M.; Lamminpää, K.; Wallenius, S.; Toppinen, S. Carbon Chain Length Increase Reactions of Platform Molecules Derived from C5 and C6 Sugars. *Ind. Eng. Chem. Res.* **2017**, *56*, 13356−13366.

(15) Boekaerts, B.; Sels, B. F. Catalytic Advancements in Carboxylic Acid Ketonization and Its Perspectives on Biomass Valorisation. *Appl. Catal., B* **2021**, *283*, 119607.

(16) Pham, T. N.; Sooknoi, T.; Crossley, S. P.; Resasco, D. E. Ketonization of Carboxylic Acids: Mechanisms, Catalysts, and Implications for Biomass Conversion. *ACS Catal.* **2013**, *3*, 2456−2473.

(17) Yang, J.; Li, N.; Li, G.; Wang, W.; Wang, A.; Wang, X.; Cong, Y.; Zhang, T. Solvent-Free Synthesis of C10and C11Branched Alkanes from Furfural and Methyl Isobutyl Ketone. *ChemSusChem* **2013**, *6*, 1149−1152.
(18) Wiegbertus Blessing, R.; Leonardus, P. Process for the Dimerisation of Levulinic Acid, Dimers Obtainable by Such Process and Esters of Such Dimers. U.S. Patent 20,060,135,793 A1, November 21, 2006.
(19) Faba, L.; Díaz, E.; Ordóñez, S. Base-Catalyzed Condensation of Levulinic Acid: A New Biorefinery Upgrading Approach. *ChemCatChem* **2016**, *8*, 1490−1494.
(20) Li, Z.; Zhang, J.; Nielsen, M. M.; Wang, H.; Chen, C.; Xu, J.; Wang, Y.; Deng, T.; Hou, X. Efficient C-C Bond Formation between Two Levulinic Acid Molecules To Produce C10 Compounds with the Cooperation Effect of Lewis and Brønsted Acids. *ACS Sustainable Chem. Eng.* **2018**, *6*, 5708−5711.
(21) Amarasekara, A. S.; Wiredu, B.; Grady, T. L.; Obregon, R. G.; Margetić, D. Solid Acid Catalyzed Aldol Dimerization of Levulinic Acid for the Preparation of C10 Renewable Fuel and Chemical Feedstocks. *Catal. Commun.* **2019**, *124*, 6−11.
(22) Melero, J. A.; Morales, G.; Iglesias, J.; Paniagua, M.; Hernández, B.; Penedo, S. Efficient Conversion of Levulinic Acid into Alkyl Levulinates Catalyzed by Sulfonic Mesostructured Silicas. *Appl. Catal., A* **2013**, *466*, 116−122.
(23) Morales, G.; Paniagua, M.; Melero, J. A.; Iglesias, J. Efficient Production of 5-Ethoxymethylfurfural from Fructose by Sulfonic Mesostructured Silica Using DMSO as Co-Solvent. *Catal. Today* **2017**, *279*, 305−316.
(24) Morales, G.; Melero, J. A.; Paniagua, M.; Iglesias, J.; Hernández, B.; Sanz, M. Sulfonic Acid Heterogeneous Catalysts for Dehydration of C6-Monosaccharides to 5-Hydroxymethylfurfural in Dimethyl Sulfoxide. *Chin. J. Catal.* **2014**, *35*, 644−655.
(25) Paniagua, M.; Melero, J. A.; Iglesias, J.; Morales, G.; Hernández, B.; López-Aguado, C. Catalytic Upgrading of Furfuryl Alcohol to Bio-Products: Catalysts Screening and Kinetic Analysis. *Appl. Catal., A* **2017**, *537*, 74−82.
(26) Russo, P. A.; Antunes, M. M.; Neves, P.; Wiper, P. V.; Fazio, E.; Neri, F.; Barreca, F.; Mafra, L.; Pillinger, M.; Pinna, N.; et al. Solid Acids with SO3H Groups and Tunable Surface Properties: Versatile Catalysts for Biomass Conversion. *J. Mater. Chem. A* **2014**, *2*, 11813−11824.
(27) Margolese, D.; Melero, J. A.; Christiansen, S. C.; Chmelka, B. F.; Stucky, G. D. Direct Syntheses of Ordered SBA-15 Mesoporous Silica Containing Sulfonic Acid Groups. *Chem. Mater.* **2000**, *12*, 2448−2459.
(28) Melero, J. A.; Stucky, G. D.; van Grieken, R.; Morales, G. Direct Syntheses of Ordered SBA-15 Mesoporous Materials Containing Arenesulfonic Acid Groups. *J. Mater. Chem.* **2002**, *12*, 1664−1670.
(29) Melero, J. A.; van Grieken, R.; Morales, G. Advances in the Synthesis and Catalytic Applications of Organosulfonic-Functionalized Mesostructured Materials. *Chem. Rev.* **2006**, *106*, 3790−3812.
(30) Zhao, D.; Feng, J.; Huo, Q.; Melosh, N.; Fredrickson, G. H.; Chmelka, B. F.; Stucky, G. D. Triblock Copolymer Syntheses of Mesoporous Silica with Periodic 50 to 300 Angstrom Pores. *Science* **1998**, *279*, 548−552.
(31) Melero, J. A.; van Grieken, R.; Morales, G.; Paniagua, M. Acidic Mesoporous Silica for the Acetylation of Glycerol: Synthesis of Bioadditives to Petrol Fuel. *Energy Fuels* **2007**, *21*, 1782−1791.
(32) Ray, W. D.; Box, G. E. P.; Hunter, W. G.; Hunter, J. S. Statistics for Experiments. An Introduction to Design, Data Analysis and Model Building. *J. R. Stat. Soc. Ser. A* **1979**, *142*, 381.

https://doi.org/10.1021/acssuschemeng.1c00378
ACS Sustainable Chem. Eng. 2021, 9, 5952−5962